

Improving the Utility of Differentially Private Clustering through Dynamical Processing

Junyoung Byun, Yujin Choi and Jaewook Lee

Abstract—This study aims to alleviate the trade-off between utility and privacy in the task of differentially private clustering. Existing works focus on simple clustering methods, which show poor clustering performance for non-convex clusters. By utilizing Morse theory, we hierarchically connect the Gaussian sub-clusters to fit complex cluster distributions. Because differentially private sub-clusters are obtained through the existing methods, the proposed method causes little or no additional privacy loss. We provide a theoretical background that implies that the proposed method is inductive and can achieve any desired number of clusters. Experiments on various datasets show that our framework achieves better clustering performance at the same privacy level, compared to the existing methods.

Index Terms—Morse theory, differential privacy, mixture of Gaussians, clustering.



1 INTRODUCTION

DIFFERENTIAL privacy (DP) provides a mathematical guarantee which can prevent the leakage of personal information from the outputs of the algorithms. DP has been successfully applied to various algorithms, from simple histogram queries [1] to complex neural networks [2]. To achieve DP, randomness should be added to the original algorithm, which generally degrades the performance. Therefore, studies on differentially private machine learning aim to preserve the performance of the algorithms as high as possible at the same level of privacy protection [3].

Clustering is widely applied in various real-world applications, such as recommendation [4], marketing [5], fraud detection [6], and image segmentation [7]. Despite its importance, there have been few studies on differentially private clustering, compared to supervised learning. Existing studies focus on relatively simple methods such as k-means clustering [8], [9], [10] or mixture of Gaussians (MoGs) [11], [12], [13]. Those methods are simple yet effective but have a limitation that they cannot express complex, nonconvex cluster structures well.

[14] applied Morse theory to improve the clustering performance of non-private support vector-based clustering algorithms. By utilizing Morse theory, their method has strength in capturing arbitrary cluster shapes. However, nonlinear support vector machines suffer in extending to a differentially private algorithm, because calculating the kernel function in their inference phase requires a set of support vectors, which is a part of training data.

To address the limitations of the previous works, in this study we propose a method to extend the existing differentially private clustering algorithms to capture more sophisticated clusters by applying Morse theory. Specifically, we utilize MoG models which do not require any information about training data after the density function

is estimated. From the MoG density function obtained as a result of differentially private clustering, we build an associated dynamical system with which we can connect the convex sub-clusters. The theoretical results demonstrate that the dynamical processing is essentially DP-friendly, hence the proposed method does not incur additional privacy loss on the existing clustering method.

2 DIFFERENTIAL PRIVACY

Differential privacy (DP) [15], [16] is a definition of privacy which offers an upper bound of mechanism changes by any change of input in a dataset.

Definition 2.1. (Differential privacy) A randomized mechanism \mathcal{M} is (ϵ, δ) -differentially private if for any set of possible outputs $\mathcal{S} \subseteq \text{Range}(\mathcal{M})$ and two neighboring datasets $D, D' \in \mathcal{D}$ which differ in exactly one data sample:

$$\Pr[\mathcal{M}(D) \in \mathcal{S}] \leq e^\epsilon \Pr[\mathcal{M}(D') \in \mathcal{S}] + \delta.$$

Remark 2.2. (Post-Processing) Let the randomized mechanism \mathcal{M} be (ϵ, δ) -differentially private. Then, for any randomized mapping f , $f \circ \mathcal{M}$ is also (ϵ, δ) -differentially private.

Remark 2.3. (Parallel Composition Theorem) Let the dataset D is partitioned by disjoint subset D_i for $i = 1, 2, \dots, n$ and let \mathcal{M}_i is ϵ_i -differentially private mechanism which takes D_i as input. Then, releasing all of the results $\mathcal{M}_1, \mathcal{M}_2, \dots, \mathcal{M}_n$ is $\max_i \epsilon_i$ -differentially private.

Other properties of DP used in this paper is in Appendix.

3 MORSE THEORY FROM A DYNAMICAL SYSTEM PERSPECTIVE

3.1 Morse theory

Let $\{x_i\} \subset \mathcal{X}$ be a given data set of N points, with $\mathcal{X} := \mathbb{R}^D$, the data space. Given a smooth real-valued function $f : \mathcal{X} \rightarrow \mathbb{R}$ mapping each point to its height, then the inverse image of a point $a \in \mathbb{R}$ called a level set can

• All authors are with the Department of Industrial Engineering, Seoul National University, Seoul 08826, Korea.
E-mail: quswons95@snu.ac.kr (Junyoung Byun), uznhigh@snu.ac.kr (Yujin Choi), jaewook@snu.ac.kr (Jaewook Lee).

Manuscript received April 19, 2005; revised August 26, 2015.

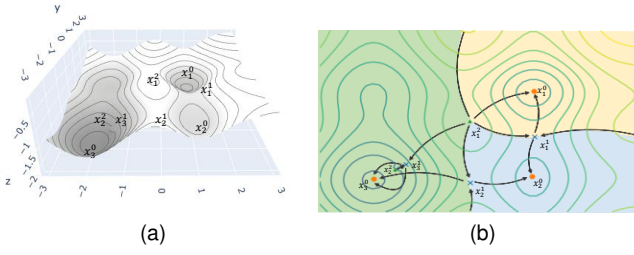


Fig. 1. Illustration of Morse theory. (b) is a level curve of (a). In (b), 'o's are stable equilibrium points, and 'x' refers to index-one equilibrium point. The triangle marker refer to index-two equilibrium point. Note that \mathbf{x}_3^1 is an index-one equilibrium vector, but not a TEV.

be decomposed into several separate connected components C_i , $i = 1, \dots, m$, i.e.,

$$\mathcal{X}_a := f^{-1}(-\infty, a] = \{\mathbf{x} \in \mathcal{X} : f(\mathbf{x}) \leq a\} = C_1 \cup \dots \cup C_m \quad (1)$$

A state vector \mathbf{x} satisfying the equation $\nabla f(\mathbf{x}) = 0$ is called an *equilibrium vector* (or *critical point*) of f . We say that an equilibrium vector \mathbf{x} of (3) is *hyperbolic* if the Hessian of f at \mathbf{x} restricted to the tangent space to \mathcal{X} at \mathbf{x} , denoted by $H_f(\mathbf{x})$, has no zero eigenvalues. Note that all the eigenvalues of the Hessian of f are real since they are real symmetric matrices. A hyperbolic equilibrium vector \mathbf{x} is called an *index- k equilibrium vector* if $H_f(\mathbf{x})$ has exactly k negative eigenvalues. The index corresponds to the dimension of the subspace consisting of directions at which f decreases. We will display the superscript k when \mathbf{x}^k is an equilibrium vector for f having index k . We call f *separating* if distinct equilibrium vectors for f have distinct functional values.

We say that f is a *Morse function* if all the equilibrium vectors of f are hyperbolic and *separating* if distinct equilibrium vectors for f have distinct functional values. A basic result of Morse theory [17], [18] is that the class of the Morse functions forms an open, dense subset of all the smooth functions in the C^2 -topology, in other words, almost all smooth functions are Morse functions. Therefore, in this paper, it is assumed that the function considered is Morse, which is "generic".

Morse theory gives the answer to the question of when the topology of $\#\mathcal{X}_a$ changes as a varies: (Here $\#\mathcal{A}$ denotes the number of connected components of a set \mathcal{A} .) See [17], [18], [19] for more details.)

- $\#\mathcal{X}_a$ increases by one, i.e. $\#\mathcal{X}_{a+\varepsilon} = \#\mathcal{X}_{a-\varepsilon} + 1$ for a sufficiently small $\varepsilon > 0$, if and only if, $a \in \{f(\mathbf{x}_1^0), \dots, f(\mathbf{x}_s^0)\}$.
- $\#\mathcal{X}_a$ decreases by one, i.e. $\#\mathcal{X}_{a+\varepsilon} = \#\mathcal{X}_{a-\varepsilon} - 1$ for a sufficiently small $\varepsilon > 0$, if and only if, $a \in \{f(\mathbf{x}_1^1), \dots, f(\mathbf{x}_t^1)\}$ and also the following Morse relation holds.

$$\begin{aligned} H_0(\mathcal{X}_{a-\varepsilon}) &\cong H_0(\mathcal{X}_{a+\varepsilon}) \oplus \mathbb{R}, \\ H_q(\mathcal{X}_{a-\varepsilon}) &\cong H_q(\mathcal{X}_{a+\varepsilon}), \quad \text{for } q > 0 \end{aligned} \quad (2)$$

where $H_q(\cdot)$ is the q -th homology space and \cong implies homotopy equivalent. Such \mathbf{x}_i^1 are called called a *transition equilibrium vector* (TEV) (Note in Figure 1, $\mathbf{x}_1^1, \mathbf{x}_2^1$ are TEVs, but \mathbf{x}_3^1 is not).

- $\#\mathcal{X}_a$ remains constant, i.e., $\#\mathcal{X}_{a+\varepsilon} = \#\mathcal{X}_{a-\varepsilon}$ for a sufficiently small $\varepsilon > 0$, if and only if, a passes the value $f(\mathbf{x}^k)$ of an index- k equilibrium vector \mathbf{x}^k with $k > 1$.

3.2 Dynamical system perspective

Morse theory in itself is not directly applicable due to the difficulty of computing the q -th homology space $H_q(\cdot)$, for example. The generalized gradient vector fields originated by [20] can help provide a way to compute it. Associated with the Morse function f , We can build the following generalized gradient system:

$$\frac{d\mathbf{x}}{dt} = -\text{grad}_R f(\mathbf{x}) \equiv -R(\mathbf{x})^{-1} \nabla f(\mathbf{x}). \quad (3)$$

where $R(\cdot)$ is a *Riemannian metric* on \mathcal{X} . (i.e. $R(\mathbf{x})$ is a positive definite symmetric matrix for all $\mathbf{x} \in \mathcal{X}$). The existence of a unique solution (or trajectory) $\mathbf{x}(\cdot) : \mathbb{R} \rightarrow \mathcal{X}$ for each initial condition $\mathbf{x}(0)$ is guaranteed by the smoothness of the function f [21], [22] (i.e. f is twice differentiable). Without loss of generality, we will assume that the trajectory $\mathbf{x}(\cdot)$ is defined on all $t \in \mathbb{R}$ for any initial condition $\mathbf{x}(0)$, which can be shown under a suitable re-parametrization [21].

A hyperbolic equilibrium vector is called a (asymptotically) *stable equilibrium vector* (or an *attractor*), denoted by \mathbf{x}^0 , if all the eigenvalues of its corresponding Jacobian are positive and an *unstable equilibrium vector* (or a *repellor*), denoted by \mathbf{x}^D , if all the eigenvalues of its corresponding Jacobian are negative. A basic result is that every local minimum of Morse function f corresponds to an (asymptotically) stable equilibrium vector of system (3). The (practical) *basin cell* of attraction of a stable equilibrium vector (SEV) \mathbf{x}^0 is the closure of an open and connected stable manifold, defined by

$$\mathfrak{B}(\mathbf{x}^0) := \text{cl}(\{\mathbf{x}(0) \in \mathcal{X} : \lim_{t \rightarrow \infty} \mathbf{x}(t) = \mathbf{x}^0\}).$$

where its boundary is denoted by $\partial\mathfrak{B}(\mathbf{x}^0)$. A basin cell groups similar data points through system (3).

Two SEVs, \mathbf{x}_i^0 and \mathbf{x}_j^0 , are said to be *adjacent* to each other if there exists an index-one equilibrium vector $\mathbf{x}_{ij}^1 \in \mathfrak{B}(\mathbf{x}_i^0) \cap \mathfrak{B}(\mathbf{x}_j^0)$. It can be shown [23], [24] that such an index-one equilibrium vector is in fact a transition equilibrium vector (TEV) between \mathbf{x}_a^0 and \mathbf{x}_b^0 that satisfies the Morse relation (2) and can therefore be computable.

4 PROPOSED METHOD

The proposed method consists of three steps. In the first step, differentially private parameters of the density function f , which is assumed to be an MoG, are estimated. Then according to Morse theory, we find TEVs of f and the density of them. Finally, we connect the adjacent centers concerning the density of the corresponding TEVs. In the rest of this chapter, we demonstrate each of the three steps in depth.

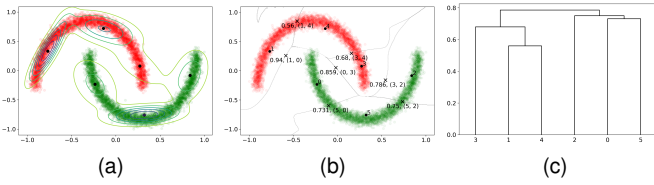


Fig. 2. Description of each step of the proposed method. (a) A mixture of six Gaussian distributions are obtained as a result of differentially private clustering ($\epsilon = 1$, $\text{ARI}=0.359$). (b) TEVs between adjacent centers are obtained, and the dissimilarity between two centers are calculated as the density of the corresponding TEV. TEVs are plotted as 'x', and the number at the bottom left of each TEV indicates its density. Two numbers in parentheses indicates which centers each TEV connects. (c) A dendrogram can be drawn according to the distance estimated in (b) ($\text{ARI}=1$ when $K=2$).

4.1 Differentially private clustering

The density function of MoG is

$$p(\mathbf{x}) = \sum_{k=1}^K \pi_k (2\pi)^{-\frac{D}{2}} |\Sigma_k|^{-\frac{1}{2}} e^{-\frac{1}{2}(\mathbf{x}-\boldsymbol{\mu}_k)^T \Sigma_k^{-1}(\mathbf{x}-\boldsymbol{\mu}_k)}, \quad (4)$$

where $\boldsymbol{\mu}_k \in \mathbb{R}^D$, $\Sigma_k \in \mathbb{R}^{D \times D}$ are the mean and the covariance of each normal distribution and π_k is the probability of belonging to the k -th cluster. Its associated MoG gradient system can be written as follows:

$$\frac{d\mathbf{x}}{dt} = R(\mathbf{x})^{-1} \nabla \ln p(\mathbf{x}) = -R(\mathbf{x})^{-1} \sum_{k=1}^K \omega_k(\mathbf{x}) \Sigma_k^{-1}(\mathbf{x} - \boldsymbol{\mu}_k), \quad (5)$$

where $R(\cdot)$ is a Riemannian metric on \mathcal{X} and

$$\omega_k(\mathbf{x}) = \frac{\pi_k (2\pi)^{-\frac{D}{2}} |\Sigma_k|^{-\frac{1}{2}} e^{-\frac{1}{2}(\mathbf{x}-\boldsymbol{\mu}_k)^T \Sigma_k^{-1}(\mathbf{x}-\boldsymbol{\mu}_k)}}{\sum_{k=1}^K \pi_k (2\pi)^{-\frac{D}{2}} |\Sigma_k|^{-\frac{1}{2}} e^{-\frac{1}{2}(\mathbf{x}-\boldsymbol{\mu}_k)^T \Sigma_k^{-1}(\mathbf{x}-\boldsymbol{\mu}_k)}} > 0.$$

This is because the majority of the studies are concentrated on k -means clustering or MoGs, from which the parameters of the Gaussian mixture can be naturally estimated.

4.1.1 Differentially private k -means clustering

There have been various studies on k -means clustering algorithms that satisfy DP [5], [8], [25], [26], [27], [28], [29]. Each method is different in privacy or utility analysis, but our method can be applied to any of them because they commonly output centers and which center each sample is allocated to. However, because k -means clustering is a kind of hard clustering, i.e., each sample is associated with a center with probability 1, it does not output the density function of the data. Therefore, we artificially build a Gaussian density function by calculating the covariance matrix of each cluster and using it as the covariance Σ_k of each Gaussian distribution. The algorithm for assigning a MoG density function to DPLloyd [25] is in Appendix.

4.1.2 Differentially private mixture of Gaussians

[11] proposed a differentially private MoG (DPMoG) method by adding noise to parameters μ_k, Σ_k, π_k in M -step of EM algorithm. Unlike k -means, in MoG each parameter is calculated using all the samples, and thus the amount of the noise added should be larger in proportion to the number

Algorithm 1 DPMoG-hard

Input: Input data $\{\mathbf{x}_n\}_{n=1}^N \in [-1, 1]^{N \times D}$, initial parameters $\{\boldsymbol{\mu}_k^0\}_{k=1}^K, \{\Sigma_k^0\}_{k=1}^K$, privacy budget (ϵ, δ) , number of iterations τ

Output: Parameters $\{\pi_k^\tau\}_{k=1}^K, \{\boldsymbol{\mu}_k^\tau\}_{k=1}^K, \{\Sigma_k^\tau\}_{k=1}^K$
 $r \leftarrow 1 + 3D + 2D^2$; $\sigma \leftarrow \sqrt{\frac{\tau}{2}} \frac{\sqrt{\log(1/\delta) + \epsilon} + \sqrt{\log(1/\delta)}}{\epsilon}$

for $k = 1$ to K **do**

$C_k \leftarrow \emptyset$

for $t = 0$ to $\tau - 1$ **do**

for $n = 1$ to N **do**

for $k = 1$ to K **do**

$$\gamma_{nk}^{t+1} \leftarrow \pi_k^t \mathcal{N}(\mathbf{x}_n | \boldsymbol{\mu}_k^t, \Sigma_k^t) / \sum_{l=1}^K \pi_l^t \mathcal{N}(\mathbf{x}_n | \boldsymbol{\mu}_l^t, \Sigma_l^t)$$

$$k^* = \arg \max_k \gamma_{nk}^{t+1}; C_{k^*} \leftarrow C_{k^*} \cup \{n\}$$

for $k = 1$ to K **do**

$$N_k \leftarrow |C_k| + \mathcal{N}(0, \sigma^2); \pi_k^{t+1} \leftarrow N_k / N; \boldsymbol{\mu}_k^{t+1} \leftarrow \frac{1}{N_k} (\sum_{n \in C_k} \mathbf{x}_n + \mathcal{N}(\mathbf{0}, \sigma^2 \mathbf{I}_D))$$

$$\Sigma_k^{t+1} \leftarrow \frac{1}{N_k} (\sum_{n \in C_k} (\mathbf{x}_n - \boldsymbol{\mu}_k^{t+1})(\mathbf{x}_n - \boldsymbol{\mu}_k^{t+1})^T + \text{sym}(\mathcal{N}(\mathbf{0}, \sigma^2 \mathbf{I}_{D(D+1)/2})))$$

of the clusters. We found that this property significantly degrades the performance. Therefore, we present a modified version of DPMoG, DPMoG-hard, whose performance is not significantly affected by the number of clusters. To enable parallel composition, we transform the responsibility obtained in E step of DPMoG so that each sample is assigned to a cluster with probability 1. This technique has been studied as hard EM [30], [31], [32], and we are the first to apply hard EM to enhance DP.

The detailed procedure of DPMoG-hard is presented in Algorithm 1. In the algorithm, writing a distribution means random sampling from that distribution. `sym` is a function that transforms a $D(D+1)/2$ -dimensional vector into a $D \times D$ -dimensional upper-triangular matrix and then copies the matrix to be symmetric. It is shown in Appendix that Algorithm 1 satisfies (ϵ, δ) -DP.

4.2 Finding transition equilibrium vectors

The main body of the proposed method is to group similar basin cells, or sub-clusters, based on mutual proximity or dissimilarity, which incorporates the ability of system (5) to generate clusters of arbitrary shapes. To incorporate Morse theory, it is necessary to find TEVs of the constructed MoG whose density serves as the dissimilarity measure.

Algorithm 2 demonstrates the procedures for finding TEVs. In the algorithm, we use the centers $\{\boldsymbol{\mu}_k\}$ obtained in the first step instead of SEPs. We exploit the fact that because the density of a center is very close to the local minimum, there exists a SEV nearby the center. Compared to previous studies, we can omit additional steps to find SEVs which requires excessive computation time. To find TEVs, we present an efficient modification of the quadratic string search method in [33], by constraining m^{t-1} from the last iteration to be the vertex of the quadratic function $y = -x^2 + x$ in the transformed coordinate where the two centers form the unit vector from the origin on the x -axis. In the transformed coordinate, we split u into $m+1$ intervals and calculate the corresponding point on the quadratic function for each vertex of the interval. Then we find the

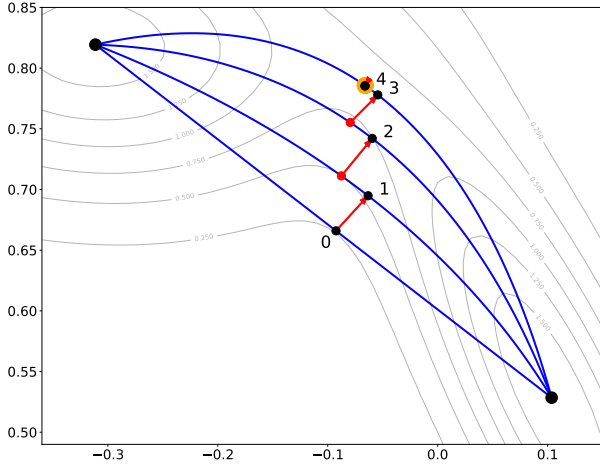


Fig. 3. Procedure to find TEVs. The big black points are the centers of MoG and the big orange point is the TEV. The small black points with numbers are m^t at step t and the small red points are the points with minimum density on the quadratic string. The red arrow means an iteration of dynamical system (5).

point with the smallest density and iterate (5) from the point for a small step size to compute m^t (line 10-13). Figure 3 illustrates the procedure of the proposed quadratic string search.

The next result shows the dynamical invariance property of the MoG system (5) that preserves differential privacy. The result indicates that Algorithm 2 does not incur any additional privacy loss.

Theorem 4.1 (Preserving Differential Privacy). *Let \mathcal{M} with $\text{Range}(\mathcal{M}) \subseteq \mathcal{X}$ be a randomized algorithm that is (ϵ, δ) -differentially private. Suppose that the Riemannian metric $R(\cdot)$ on \mathcal{X} of the associated MoG gradient system (5) has a finite condition number. Then the inductive dynamical processing (5) applied to \mathcal{M} is (ϵ, δ) -differentially private, i.e. the solution trajectory $\mathbf{x}(t)$ of the MoG gradient system (5) with initial condition $\mathbf{x} \in \mathcal{M}$ is (ϵ, δ) -differentially private.*

Proof. See Appendix. \square

4.3 Hierarchical merging of sub-clusters

The last step is a modified version of Kruscal's algorithm for minimum cost-spanning tree. The method begins with every SEV representing a singleton cluster. Denote these clusters $C_1 = \{\mathbf{x}_1^0\}, \dots, C_L = \{\mathbf{x}_L^0\}$. At each of the $L - 1$ steps the closest two clusters (i.e., two separate clusters containing two adjacent SEVs with the least edge weight distance) are merged into a single cluster, producing one less cluster at the next higher level. This process is terminated when we get K clusters starting from L clusters. The detailed procedure is demonstrated in Algorithm 3. Because Algorithm 3 works with only the centers and the TEVs which preserve DP, it naturally preserves (ϵ, δ) -DP by post-processing property.

Another distinguished feature of the MoG system (5) is the agglomerative property, i.e. system (5) enables us to build a hierarchy of clusters starting from the basin cells. This ensures that Algorithm 3 can obtain any desired number of clusters.

Algorithm 2 Finding Transition Equilibrium Vectors

- 1: **Input:** Centers $\{\mu_k\}_{k=1}^K$, density function f , line search parameter m , number of iterations τ
- 2: **Output:** Set of tuples T , which consists of adjacent centers and corresponding TEV
- 3: $T \leftarrow \emptyset$
- 4: $TPs \leftarrow \emptyset$ // Set of candidate transition points
- 5: **for** $k = 1$ to K **do**
- 6: **for** $l = k + 1$ to K **do**
- 7: $i^* \leftarrow \arg \max_{i \in \{1, \dots, m\}} f(\mu_k + \frac{i}{m+1}(\mu_l - \mu_k))$
- 8: $m^0 \leftarrow \mu_k + \frac{i^*}{m+1}(\mu_l - \mu_k)$; $m^0 \leftarrow$ Numerically integrate (3) from m^0
- 9: **for** $t = 1$ to τ **do**
- 10: $\mathbf{u} \leftarrow \mu_l - \mu_k$; $\mathbf{v} \leftarrow m^{t-1} - \mu_k$
- 11: $i^* \leftarrow \arg \min_{i \in \{1, \dots, m\}} f(\mu_k + \frac{i}{m+1}\mathbf{u} + (\frac{i}{m+1} - (\frac{i}{m+1})^2)(4\mathbf{v} - 2\mathbf{u}))$
- 12: $m^t \leftarrow \mu_k + \frac{i^*}{m+1}\mathbf{u} + (\frac{i^*}{m+1} - (\frac{i^*}{m+1})^2)(4\mathbf{v} - 2\mathbf{u})$
- 13: $m^t \leftarrow$ Numerically integrate (3) from m^t
- 14: $t_{tmp} \leftarrow$ Find the solution of $\nabla f(\mathbf{x}) = 0$ from m^t ; $TPs \leftarrow TPs \cup \{t_{tmp}\}$
- 15: **for** $t \in TPs$ **do**
- 16: **if** Hessian $\nabla^2 f(t)$ has one negative eigenvalue **then**
- 17: $e \leftarrow$ Eigenvector corresponding to the negative eigenvalue
- 18: $\mathbf{x}_0 \leftarrow t + \epsilon e$; $\mathbf{x}_1 \leftarrow t - \epsilon e$ for small $\epsilon > 0$
- 19: $\mu_0, \mu_1 \leftarrow$ Numerically integrate (3) from $\mathbf{x}_0, \mathbf{x}_1$
- 20: **if** $\mu_0 \neq \mu_1$ **then**
- 21: $T \leftarrow T \cup \{(\mu_0, \mu_1, f(t))\}$

Algorithm 3 Hierarchically Merging Sub-clusters

- Input:** Set of Tuples T , number of clusters K
- Output:** Clusters $\{C\}_{k=1}^K$
- $L \leftarrow |V|$
- $C_1 \leftarrow \{\mu_1\}, \dots, C_L \leftarrow \{\mu_L\}$ // Set initial clusters
- // Set initial distances
- if** $\langle \mu_i, \mu_j, f(t) \rangle \in T$ **then**
- $d(C_i, C_j) \leftarrow f(t)$
- else**
- $d(C_i, C_j) \leftarrow \infty$
- for** $l = 1$ to $L - K$ **do**
- Find the smallest d and the corresponding C_a, C_b
- $C_{L+l} \leftarrow C_a \cup C_b$
- $d(C_{L+l}, C_c) \leftarrow \min\{d(C_a, C_c), d(C_b, C_c)\}$ for all remaining C_c s
- Remove C_a and C_b

Theorem 4.2 (Agglomerative Property). *Let $\mathbf{x}_i^0, i = 1, \dots, s$ and $\mathbf{x}_j^1, j = 1, \dots, t$ be the SEVs and the TEVs of the MoG system (5), respectively. Consider an agglomerative process such that each basin cell $\mathfrak{B}(\mathbf{x}_i^0)$ starts in its own cluster and a pair of clusters are merged when the two separate clusters contain adjacent basin cells with the least edge weight $f(\mathbf{x}_j^1)$. Then the merging occurs when we decrease the level value a starting from $\max_i f(\mathbf{x}_i^0)$ until it hits the value in $\{f(\mathbf{x}_1^1), \dots, f(\mathbf{x}_t^1)\}$ and this process is terminated when we get one cluster, say \mathcal{X} , starting from s clusters.*

Proof. See Appendix. \square

We refer the readers to Appendix for the utility bound

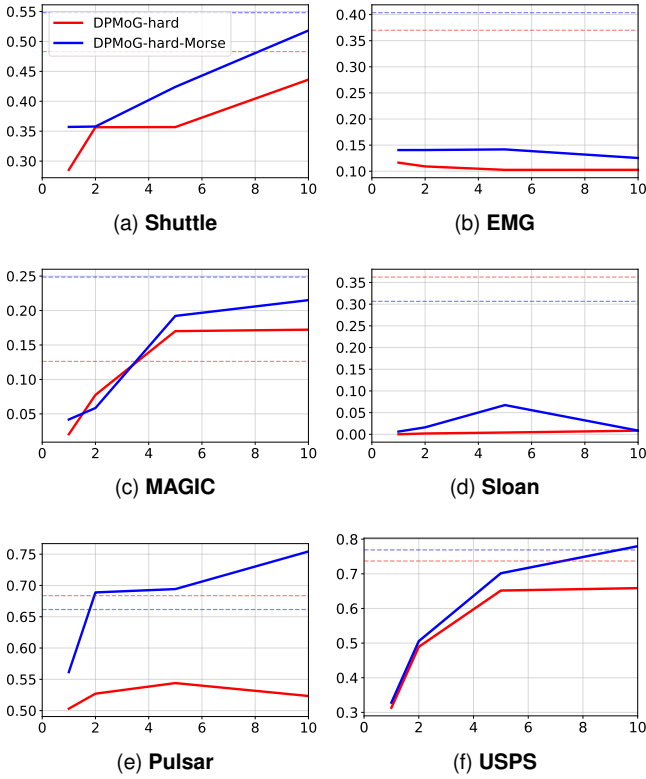


Fig. 4. Clustering results for real-world datasets. The x-axis indicates the noise budget ϵ , and the y-axis indicates the ARI score. The dotted lines indicate the performances of the non-private models.

of the proposed method, which demonstrates that applying Morse theory improves the generalization error.

5 EXPERIMENTS

We evaluate the proposed method on six real-world datasets, which aims to verify that our method achieves better clustering results compared to the existing methods.

5.1 Details on experiments

To compare the utility of differentially private clustering methods before and after applying Morse theory, we compared **DPMoG-hard** and **DPMoG-hard-Morse**, where “-Morse” denotes that Morse theory was applied. For clustering metric, we used adjusted Rand index (ARI). ARI has a value between 0 and 1, and the closer the value is to 1, the better the clustering is. Although true labels are needed to compute ARI, we found out existing clustering metrics that do not require true labels, such as silhouette score, do not increase by capturing complex shape of clusters because those metrics are suitable to fit convex cluster shapes.

Total privacy budget ϵ was set in $\{10, 5, 2, 1\}$. For $\epsilon < 1$, **DPMoG-hard** showed meaningless ARI scores for most of the datasets. This result is different from the experiments using other metrics such as the k-means objective, in which performance is preserved for smaller ϵ . Also, the level of privacy can be further enhanced by using more advanced models. The experiments were performed with Python 3.6.9, and all experiments were repeated 5 times and the average of the results was obtained. A more detailed explanation of the parameters used for the experiments is in Appendix.

TABLE 1
ARI scores with different numbers of initial sub-clusters for **Pulsar** dataset.

| $\epsilon \backslash K_0$ | 6 | 10 | 15 | 20 |
|---------------------------|----------|----------|----------|----------|
| 10 | 0.754277 | 0.754838 | 0.766507 | 0.728404 |
| 5 | 0.694178 | 0.673453 | 0.659280 | 0.664384 |
| 2 | 0.688862 | 0.610148 | 0.596477 | 0.576486 |
| 1 | 0.561494 | 0.584608 | 0.577082 | 0.542264 |

5.2 Results

5.2.1 Effectiveness of Morse theory

Figure 4 demonstrates the clustering results for the six datasets. As shown in the figure, by applying Morse theory **DPMoG-hard-Morse** shows higher ARI than **DPMoG-hard** in all cases. Specifically, for **Pulsar** dataset, ARI increased by up to 0.2, which means a significant improvement in the utility. For other datasets, ARI generally increased by 0.05 to 0.1. The results imply that the proposed method can effectively group the generated sub-clusters to express the clusters of arbitrary shapes.

Meanwhile, for most data, the difference between ARI scores of **DPMoG-hard** and **DPMoG-hard-Morse** tends to decrease as epsilon gets smaller. Also, for **EMG** and **Sloan** datasets, the increase was relatively small for all ϵ . Both datasets in common show poor performance compared to the non-private model even at $\epsilon = 10$. Combining these facts, it is a limitation of the proposed method that applying Morse theory does not have a significant effect when the performance of the baseline model is completely degraded because the noise to guarantee DP is too large. However, **DPMoG-hard** is a relatively simple model, and this limitation can be overcome by using a better baseline model. Results with more base methods, which includes recent k-means clustering methods [8], [34], are in Appendix.

5.2.2 Effect of increasing sub-clusters

Table 1 shows the clustering results with different numbers of initial sub-clusters, for **Pulsar** dataset. The clustering performance tends to decrease as K_0 increases. The result can be interpreted in two ways. First, the difference in performance can be caused by the increase in the number of TEVs. Another interpretation is that the increase in the number of sub-clusters reduces the number of samples belonging to each cluster, and thus the influence of noise increases.

6 RELATED WORKS

[26] used local sensitivity to lower the magnitude of the noise added to ensure DP, and proposed sample-and-aggregate framework and applied it to k-means clustering. [27] proposed a method to compute differentially private coresets for k-means and k-median clustering. [8] presented a non-interactive differentially private k-means clustering method called EUGkM, and enhanced its utility by using a hybrid approach of DPLloyd and EUGkM. Recently, studies on differentially private k-means clustering algorithms focus on improving sample-and-aggregate framework. [28],

[29], [35] proposed an improved framework on well separated dataset, with better DP guarantees and sample complexity bounds. The method in [28] is also applied to MoG.

As in the studies of k-means clustering, [12] presented a sample-and-aggregate framework on MoG, further reducing the effect of noise with principal component analysis. In addition to k-means clustering and MoG, several clustering algorithms with DP are being studied. [36], [37] studied differentially private DBSCAN algorithms. Recently, [38] proposed a differentially private fuzzy k-means algorithm with gaussian kernel function.

7 CONCLUSION

We proposed an effective differentially private clustering method, which utilizes Morse theory to express complex, nonconvex clusters without sacrificing privacy. The proposed method first generates many convex sub-clusters using mixture of Gaussians or k-means clustering, and hierarchically connects the sub-clusters using a hierarchical procedure based on Morse theory. Experimental results ensure that applying Morse theory improves clustering utility for various baseline methods at the same privacy levels.

APPENDIX A MIXTURE OF GAUSSIANS

For a D -dimensional data point \mathbf{x} , the density function of mixture of Gaussians (MoG) model can be written as a linear combination of normal distributions:

$$p(\mathbf{x}) = \sum_{k=1}^K \pi_k \mathcal{N}(\mathbf{x} | \boldsymbol{\mu}_k, \boldsymbol{\Sigma}_k)$$

where $\boldsymbol{\mu}_k \in \mathbb{R}^D$, $\boldsymbol{\Sigma}_k \in \mathbb{R}^{D \times D}$ are the mean and the covariance of each normal distribution. MoG is demonstrated as a latent variable model, by introducing a discrete variable $\mathbf{z} \in \{0, 1\}^K$ whose k -th element $z_k = 1$ if \mathbf{x} belongs to k -th cluster and 0 else. Then $\pi_k \in \mathbb{R}$ can be interpreted as the marginal distribution of \mathbf{z} , such that $\pi_k = p(z_k = 1)$.

Like other latent variable models, the likelihood of MoG is maximized via EM algorithm. In E-step, the responsibility $\gamma(z_{nk}) = p(z_{nk} = 1 | \mathbf{x}_n)$ is estimated according to the current parameters. In M-step, The parameters are updated according to the responsibility.

- (E-step) The responsibility $\gamma(z_{nk}) = p(z_{nk} = 1 | \mathbf{x}_n)$ is estimated according to current parameters:

$$\gamma(z_{nk}) = \frac{\pi_k \mathcal{N}(\mathbf{x}_n | \boldsymbol{\mu}_k, \boldsymbol{\Sigma}_k)}{\sum_{l=1}^K \pi_l \mathcal{N}(\mathbf{x}_n | \boldsymbol{\mu}_l, \boldsymbol{\Sigma}_l)}$$

- (M-step) The parameters are updated according to the responsibility:

$$\begin{aligned} \boldsymbol{\mu}_k &= \frac{1}{N_k} \sum_{n=1}^N \gamma(z_{nk}) \mathbf{x}_n \\ \boldsymbol{\Sigma}_k &= \frac{1}{N_k} \sum_{n=1}^N \gamma(z_{nk}) (\mathbf{x}_n - \boldsymbol{\mu}_k) (\mathbf{x}_n - \boldsymbol{\mu}_k)^T \\ \pi_k &= \frac{N_k}{N} \end{aligned}$$

where N is the number of data points and $N_k = \sum_{n=1}^N \gamma(z_{nk})$.

It is known that by restricting $\boldsymbol{\Sigma}_k = \alpha \mathbf{I}$ for all k , MoG reduces to k-means clustering when $\alpha \rightarrow \infty$.

APPENDIX B PROPERTIES OF EQUILIBRIUM VECTORS

[20] shows that system (3) is arbitrarily close to a C^∞ -vector field and satisfies the transversality conditions on the equilibrium vectors. Also all the generalized gradient system have the equilibrium vectors at the same locations with the same index, i.e., if $R_1(\mathbf{x})$ and $R_2(\mathbf{x})$ are Riemannian metrics on \mathbb{R}^D , then the locations and the indices of the equilibrium vectors of $\text{grad}_{R_1} f(\mathbf{x})$ and $\text{grad}_{R_2} f(\mathbf{x})$ are the same. This property helps design computationally efficient algorithms.

APPENDIX C DIFFERENTIAL PRIVACY OF THE PROPOSED METHOD

Definition C.1. (Sensitivity) For a function f ,

$$\Delta_p f = \max_{D, D'} \|f(D) - f(D')\|_p$$

is called a ℓ_p -sensitivity of f . ℓ_2 -sensitivity is commonly used in (ϵ, δ) -differential privacy.

Then Algorithm 1 can be proved to satisfy (ϵ, δ) -DP with composition properties of zero-centered DP (zCDP) [39]. Below we introduce some properties of zCDP.

Remark C.2. (Proposition 1.3 [39]) If \mathcal{M} satisfies ρ -zCDP, then \mathcal{M} satisfies $(\rho + 2\sqrt{\rho \log(1/\delta)}, \rho)$ DP for any $\delta > 0$.

Remark C.3. (Proposition 1.4 [39]) If \mathcal{M} satisfies ϵ -DP, then \mathcal{M} satisfies $\frac{1}{2}\epsilon^2$ -zCDP.

Remark C.4. (Proposition 1.6 [39]) Let function $f : \mathcal{X}^n \rightarrow \mathbb{R}$ has a sensitivity Δ . Then on input x , releasing a sample from $\mathcal{N}(f(x), \sigma^2)$ satisfies $(\Delta^2/2\sigma^2)$ -zCDP.

Remark C.5. (Lemma 1.8 [39]) Let randomized mechanisms \mathcal{M}_1 and \mathcal{M}_2 satisfy ρ_1 -zCDP and ρ_2 -zCDP, respectively. Then the mapping $\mathcal{M}_{1,2} = (\mathcal{M}_1, \mathcal{M}_2)$ satisfies $(\rho_1 + \rho_2)$ -zCDP.

The sensitivity of N_k is 1, and the sensitivity of each coordinate of $\sum_{n \in C_k} \mathbf{x}_n$ is 2. $\sum_{n \in C_k} \mathbf{x}_n \mathbf{x}_n^T$ has $D(D+1)/2$ unique elements, among which D diagonal elements have sensitivity 1 and the other $D(D-1)/2$ elements have sensitivity 2. Using remark C.4 and C.5, N_k is $(1/2\sigma^2)$ -zCDP, $\sum_{n \in C_k} \mathbf{x}_n$ (plus noise) is $(2^2 D/2\sigma^2)$ -zCDP, and $\sum_{n \in C_k} \mathbf{x}_n \mathbf{x}_n^T$ (plus noise) is $(D/2\sigma^2)$ -zCDP for diagonal elements and $(2^2 D(D-1)/4\sigma^2)$ -zCDP for the others for an iteration. Because $\pi_k, \boldsymbol{\mu}_k, \boldsymbol{\Sigma}_k$ can be calculated with these three terms, by remark C.5, τ iterations of the algorithm results in $(1 + 3D + 2D^2)\tau/2\sigma^2$ -zCDP. According to remark C.2, the algorithm 1 is (ϵ, δ) -DP with $\sigma = \frac{\sqrt{\tau\tau} \sqrt{\log(1/\delta) + \epsilon} + \sqrt{\log(1/\delta)}}{\epsilon}$, where $r = 1 + 3D + 2D^2$.

Algorithm 4 DPLloyd-MoG

Input: Input data $\{\mathbf{x}_n\}_{n=1}^N \in [-1, 1]^{N \times D}$, number of cluster K , privacy budget (ϵ, δ) , number of iterations τ .

Output: Parameters $\{\pi_k\}_{k=1}^K, \{\mu_k\}_{k=1}^K, \{\Sigma_k\}_{k=1}^K$
 $\{\mu_1, \mu_2, \dots, \mu_K\} \leftarrow$ Randomly generate D dimensional points from uniform distribution
 $r \leftarrow (2D + 1)^2 \tau^2 + D(2D - 1)$
 $\sigma \leftarrow \sqrt{\frac{r}{2} \sqrt{\log(1/\delta) + \epsilon} + \sqrt{\log(1/\delta)}}$
while iterate until τ times **do**
 for $k = 1$ to K **do**
 $C_k \leftarrow \{\mathbf{x}_n : \|\mathbf{x}_n - \mu_k\| \leq \|\mathbf{x}_n - \mu_i\|, \forall 1 \leq i \leq k\}$
 $N_k \leftarrow |C_k| + \text{Lap}(\sigma, \text{size} = 1)$
 $\mu_k \leftarrow \frac{1}{N_k} (\sum_{n \in C_k} \mathbf{x}_n + \text{Lap}(\sigma, \text{size} = D))$
 for $k = 1$ to K **do**
 $\pi_k \leftarrow N_k / N$
 $\Sigma_k^T \leftarrow \frac{1}{N_k} (\sum_{n \in C_k} (\mathbf{x}_n - \mu_k)(\mathbf{x}_n - \mu_k)^T + \text{sym}(\mathcal{N}(\mathbf{0}, \sigma^2 \mathbf{I}_{D(D+1)/2})))$

APPENDIX D
ASSIGNING MOG DENSITY FUNCTION TO DPLLLOYD

As mentioned in the paper, k-means clustering is a hard clustering method which does not output the density function. Thus, we calculated the covariance of each cluster for MoG density function. Because we have to add noise when calculating covariance matrices to ensure DP, it causes a little additional privacy loss.

Algorithm 4 is the pseudo-code of DPLloyd algorithm with covariance. In the algorithm, the privacy budget was assigned so that every noise has the same parameter σ . Though there are infinitely many privacy-assigning strategies, our strategy empirically resulted in a relatively good clustering results. Similar to Algorithm 1, we can easily show that the Algorithm 4 is (ϵ, δ) -differentially private, using remark C.2 to C.5.

APPENDIX E
MORE THEORETICAL RESULTS

With the aid of the adjacent SEVs and TEVs, we can build the following weighted graph $G = (V, E)$ as in [19]:

1. The vertices V of G are the SEVs, $\mathbf{x}_1^0, \dots, \mathbf{x}_s^0$, $i = 1, \dots, s$ of (3).
2. The edge E of G can only connect vertices of adjacent SEVs, say $\mathbf{x}_i^0, \mathbf{x}_j^0$ with the edge weight, $d_E(\mathbf{x}_i^0, \mathbf{x}_j^0) := f(\mathbf{x}_{ij}^1)$ where \mathbf{x}_{ij}^1 is a TEV between \mathbf{x}_i^0 and \mathbf{x}_j^0 .

Corresponding to \mathcal{X}_a , we can then build a sub-graph of G , denoted by $G_a = (V_a, E_a)$ with the following elements:

1. The vertices $V_a \subset V$ of G_a consists of SEVs, \mathbf{x}_i^0 , in V with $f(\mathbf{x}_i^0) < a$.
2. The edge $E_a \subset E$ of G_a consists of $(\mathbf{x}_i^0, \mathbf{x}_j^0) \in E$ with $d_E(\mathbf{x}_i^0, \mathbf{x}_j^0) < a$.

The next result establishes the dynamical property of the graph G_a showing the equivalence of the topological structures of G_a and the connected components of \mathcal{X}_a .

Proposition E.1. [40] *With respect to the MoG (4), \mathbf{x}_i^0 and \mathbf{x}_j^0 are in the same connected component of the sub-graph G_a if, and*

only if, \mathbf{x}_i^0 and \mathbf{x}_j^0 are in the same cluster of the level set \mathcal{X}_a , that is, each connected component of G_a corresponds to a cluster of \mathcal{X}_a .

One distinguished feature of the MoG system (5) is the complete stability, i.e. every trajectory converges one of the SEVs almost surely when system (5) is applied. Although the traditional density-based clustering methods try to assign the same label to the point in the same connected component C_i , they need retraining to assign a label to a new test point, which wastes privacy budget. The next result shows an inductive property of system (5), which provides a way to assign a label to a new test point without retraining.

Theorem E.2 (Inductive Property). *Suppose that the Riemannian metric $R(\cdot)$ on \mathcal{X} of the associated MoG gradient system (5) has a finite condition number. Then the whole data space are almost surely pairwise disjoint union of the basin cells $\mathfrak{B}(\mathbf{x}_i^0)$ where $\mathbf{x}_i^0, i = 1, \dots, s$ are the SEVs of system (5), i.e.*

$$\mathcal{X} = \mathfrak{B}(\mathbf{x}_1^0) \dot{\cup} \dots \dot{\cup} \mathfrak{B}(\mathbf{x}_s^0)$$

Here almost surely disjoint union $A \dot{\cup} B$ of two nonempty sets A and B means that $A \cap B$ has a Lebesgue measure zero.

Proof. Following the proof of Lasalle's invariance property theorem as in [21], [41], it can be easily shown that every bounded trajectory of system (5) converges to one of the equilibrium vectors. Therefore it is enough to show that every trajectory is bounded.

Since $R(\mathbf{x})^{-1}$ and Σ_k^{-1} are positive definite, we can let $A_k(\mathbf{x})$ be the Cholesky factorization of the positive definite matrix $R(\mathbf{x})^{-1} \Sigma_k^{-1}$ that satisfies $R(\mathbf{x})^{-1} \Sigma_k^{-1} = A_k(\mathbf{x})^T A_k(\mathbf{x})$. Then $(\mathbf{x}^T R(\mathbf{x})^{-1} \Sigma_k^{-1} \mathbf{x}) = \|A_k(\mathbf{x}) \mathbf{x}\|^2$. Since the condition number of $R(\mathbf{x})$ is bounded, by the spectral theorem, there exist positive smooth eigenvalue functions $\lambda_{\min}^k(\mathbf{x}), \lambda_{\max}^k(\mathbf{x}) > 0$ and $\gamma > 0$ such that

$$\|A_k(\mathbf{x})\| = \sqrt{\lambda_{\max}^k(\mathbf{x})}, \quad \forall k = 1, \dots, K, \quad \forall \mathbf{x} \in \mathcal{X},$$

$$\kappa(A_k(\mathbf{x})) := \left(\lambda_{\max}^k(\mathbf{x}) / \lambda_{\min}^k(\mathbf{x}) \right)^{1/2} \leq \gamma, \quad \forall k = 1, \dots, K, \quad \forall \mathbf{x} \in \mathcal{X}$$

where $\|\cdot\|$ denotes the Euclidean norm or ℓ_2 -norm. Now let $V(\mathbf{x}) = \frac{1}{2} \|\mathbf{x}\|^2$ and choose $\Upsilon > \gamma \max_k \| \mu_k \|$. Then for any $L > \Upsilon$, and for all $\|\mathbf{x}\| = L$, we have

$$\begin{aligned} \frac{\partial}{\partial t} V(\mathbf{x}) &= \mathbf{x}^T \frac{d\mathbf{x}}{dt} = -\mathbf{x}^T \sum_k \omega_k(\mathbf{x}) R(\mathbf{x})^{-1} \Sigma_k^{-1} (\mathbf{x} - \mu_k) \\ &= -\mathbf{x}^T \sum_k \omega_k(\mathbf{x}) R(\mathbf{x})^{-1} \Sigma_k^{-1} \mathbf{x} + \mathbf{x}^T \sum_k \omega_k(\mathbf{x}) R(\mathbf{x})^{-1} \Sigma_k^{-1} \mu_k \\ &= -\sum_k \omega_k(\mathbf{x}) \mathbf{x}^T A_k(\mathbf{x})^T A_k(\mathbf{x}) \mathbf{x} + \sum_k \omega_k(\mathbf{x}) \mathbf{x}^T A_k(\mathbf{x})^T A_k(\mathbf{x}) \mu_k \\ &\leq -\sum_k \omega_k(\mathbf{x}) \|A_k(\mathbf{x}) \mathbf{x}\|^2 + \sum_k \omega_k(\mathbf{x}) \|A_k(\mathbf{x}) \mathbf{x}\| \|A_k(\mathbf{x}) \mu_k\| \\ &= \sum_k \omega_k(\mathbf{x}) \|A_k(\mathbf{x}) \mathbf{x}\| (\|A_k(\mathbf{x}) \mu_k\| - \|A_k(\mathbf{x}) \mathbf{x}\|) \\ &\leq \sum_k \omega_k(\mathbf{x}) \|A_k(\mathbf{x}) \mathbf{x}\| (\sqrt{\lambda_{\max}^k(\mathbf{x})} \|\mu_k\| - \sqrt{\lambda_{\min}^k(\mathbf{x})} \|\mathbf{x}\|) \\ &< 0 \end{aligned}$$

Therefore, for any $L > \Upsilon$, the trajectory starting from any point on $\|\mathbf{x}\| = L > \Upsilon$ always enters into the bounded set $\|\mathbf{x}\| \leq L$, which implies that $\{\mathbf{x}(t) : t \geq 0\}$ is bounded. \square

This result naturally partitions the sample space by assigning points belonging to different basin cells to their

respective SEVs. Moreover, it is computationally feasible to identify a basin cell of a SEV by applying the system (5).

APPENDIX F PROOF OF THEOREMS

F.1 Proof of Theorem 4.1

Let \mathcal{M} with $\text{Range}(\mathcal{M}) \subseteq \mathcal{X}$ be a randomized algorithm that is (ϵ, δ) -differentially private. Then under the same condition of Theorem E.2, the inductive dynamical processing by (5) applied to \mathcal{M} is (ϵ, δ) -differentially private, i.e. the solution trajectory $\mathbf{x}(t)$ of the MoG gradient system (5) with initial condition $\mathbf{x}(0) = \mathbf{x} \in \mathcal{M}$ is (ϵ, δ) -differentially private.

Proof. Define the flow $\Phi_t : \mathcal{X} \rightarrow \mathcal{X}$ of the MoG gradient system (5) by $\Phi_t(\mathbf{x}) = \mathbf{x}(t)$ with initial condition $\mathbf{x}(0) = \mathbf{x}$ for $t \in \mathbb{R}$. Then by the fundamental theorem of the flow defined by system (5), we have $\Phi_{s+t}(\mathbf{x}) = \Phi_s \circ \Phi_t(\mathbf{x})$ for all $\mathbf{x} \in \mathcal{X}$ and $s, t \in \mathbb{R}$. (See [41], [42] for more details.) Now let a pair of neighboring databases D_1, D_2 with $\|D_1 - D_2\|_1 \leq 1$ be given. Then for all $\mathbf{x} \in \mathcal{M}(D_1)$

$$\mathbf{x}(t) = \Phi_t \circ \Phi_0(\mathbf{x}) = \Phi_t \circ \mathbf{x}(0)$$

For any event $\mathcal{O} \subset \text{Range}(\mathcal{M}) \subseteq \mathcal{X}$ and any $t \in \mathbb{R}$, we let $\mathcal{W}_t = \{\mathbf{x} \in \mathcal{X} : \mathbf{x}(t) \in \mathcal{O}\}$. Then we have

$$\begin{aligned} \Pr\{\mathbf{x}(t) \in \mathcal{O} : \mathbf{x} \in \mathcal{M}(D_1)\} &= \Pr\{\mathcal{M}(D_1) \in \mathcal{W}_t\} \\ &\leq e^\epsilon \Pr\{\mathcal{M}(D_2) \in \mathcal{W}_t\} + \delta \\ &= e^\epsilon \Pr\{\mathbf{x}(t) \in \mathcal{O} : \mathbf{x} \in \mathcal{M}(D_2)\} + \delta \end{aligned}$$

Since this result works for any $t \in \mathbb{R}$, the inductive dynamical processing applied to \mathcal{M} by system (5) is (ϵ, δ) -differentially private. \square

F.2 Proof of Theorem 4.2

Let $\mathbf{x}_i^0, i = 1, \dots, s$ and $\mathbf{x}_j^1, j = 1, \dots, t$ be the SEVs and the TEVs of the MoG system (5), respectively. Consider an agglomerative process such that each basin cell $\mathfrak{B}(\mathbf{x}_i^0)$ starts in its own cluster and a pair of clusters are merged when the two separate clusters contain adjacent basin cells with the least edge weight $f(\mathbf{x}_j^1)$. Then the merging occurs when we decrease the level value a starting from $\max_i f(\mathbf{x}_i^0)$ until it hits the value in $\{f(\mathbf{x}_1^1), \dots, f(\mathbf{x}_t^1)\}$ and this process is terminated when we get one cluster, say \mathcal{X} , starting from s clusters.

Proof. The first part of the proof comes from the Morse theory. For the second part of the proof, it is sufficient to show that $\eta > 0$ exists, with \mathcal{X}_r connected for all $0 < r < \eta$. From the Cholesky factorization of Σ_k^{-1} , we can let $\Sigma_k^{-1} = U_k^T U_k$ where U_k is an upper triangle matrix with positive diagonal elements. By the singular value decomposition theorem, $0 < \sigma_d^{(k)} \|\mathbf{x}\| \leq \|U_k \mathbf{x}\| \leq \sigma_1^{(k)} \|\mathbf{x}\|$ where $\sigma_1^{(k)} \geq \dots \geq \sigma_d^{(k)}$ are the singular values for $k = 1, \dots, K$. Let $a := \min_k \sigma_d^{(k)}$, $b := \max_k \sigma_1^{(k)}$. Choose $\zeta > \max\{\frac{b}{a}, \gamma\} \cdot \max_k \|\boldsymbol{\mu}_k\|$, then for all $\|\mathbf{x}\| = L > \zeta$, we have

$$\|U_k(\mathbf{x} - \boldsymbol{\mu}_k)\| \leq \|U_k \mathbf{x}\| + \|U_k \boldsymbol{\mu}_k\| < bL + \frac{a\sigma_1^{(k)}}{b} L \leq (b+a)L,$$

By the proof of Theorem E.2, every trajectory starting from $\|\mathbf{x}\| = L$ for any $L > \zeta$ always enters into the $S_L := \{\mathbf{x} : \|\mathbf{x}\| \leq L\}$, which is a connected and bounded

set. It is enough to show that there exist a $\eta > 0$ such that $S_L \subset \mathcal{X}_\eta$.

$$\begin{aligned} p(\mathbf{x}) &= \sum_{k=1}^K \pi_k (2\pi)^{-\frac{d}{2}} |\boldsymbol{\Sigma}_k|^{-\frac{1}{2}} e^{-\frac{1}{2}(\mathbf{x} - \boldsymbol{\mu}_k)^T \boldsymbol{\Sigma}_k^{-1} (\mathbf{x} - \boldsymbol{\mu}_k)} \\ &> \sum_{k=1}^K \pi_k (2\pi)^{-\frac{d}{2}} |U_k| e^{-\frac{1}{2}(a+b)^2 L^2} \\ &\geq \min_k |U_k| (2\pi)^{-\frac{d}{2}} e^{-\frac{1}{2}(a+b)^2 L^2} \\ &\geq (2\pi/a^2)^{-\frac{d}{2}} e^{-\frac{1}{2}(a+b)^2 L^2}. \end{aligned}$$

The second inequality follows from $\sum_{k=1}^K \pi_k = 1$, and the last inequality follows from

$$|U_k| = \prod_{i=1}^d \sigma_i^{(k)} \geq (\sigma_d^{(k)})^d \geq a^d$$

When we choose $\eta = (2\pi/a^2)^{-\frac{d}{2}} e^{-\frac{1}{2}(a+b)^2 L^2}$, we have $S_L \subset \mathcal{X}_r$ for all $0 < r < \eta$. Hence, by theorem E.2, for any point $\mathbf{x}_0 \in (\mathcal{X}_r \setminus S_L)$, every trajectory starting from \mathbf{x}_0 should hit the boundary L and enters into the region S_L . This implies that the set S_L is a strong deformation retract of the level set \mathcal{X}_r , which shows that \mathcal{X}_r is connected for all $r < \gamma$. \square

APPENDIX G MORSE THEORY IMPROVES UTILITY

We follow a definition of density-based clusters that describes ‘‘region of relatively high density $p(\cdot)$ ’’ proposed by [43] and [44] where the cluster assumption involves connected components of the level set $\{x : p(x) \geq \rho\}$ for some $\rho > 0$. This definition in addition to Proposition E.1 and Theorem 4.2, motivates us to construct a generalization error bounded by

$$\mathbb{P}\{x : p(x) \leq \rho - \gamma\} + d_H(\mathcal{K}, \mathcal{K}'),$$

for any $\gamma > 0$ where $d_H(\mathcal{K}, \mathcal{K}')$ is the divergence measuring the discrepancy between the actual connected components \mathcal{K} determined by the set $\{x : p(x) \geq \rho\}$ and the (wrongly assigned) cluster sets \mathcal{K}' , similar to the measures of impurity. The first term of the generalization error bound denotes a probability that training sample does not belong to the induced decision region. Despite the first term is generally used in density-based clustering problems, it is not sufficient since it does not consider whether the connected components (sub-clusters in this paper) is well identified. Thus, we added the second term to measure the error between the (wrongly) assigned clusters and the actual connected components. Our Proposition E.1 implies that the constructed graph in the proposed method can appropriately capture the connected components, and Theorem 4.2 ensures that the proposed method can find desirably connected clusters for any level ρ . This results implies that the second term becomes tighter than other existing MoG clustering methods when the Morse theory is applied. Since the first term of the generalization bound does not change whether applying Morse theory or not, the proposed method gives a tighter generalization bound.

Note that any generalization error bound of the first term is applicable to any density function, so it can be used regardless of whether the MoG algorithm satisfies differential

TABLE 2
Description of datasets.

| Dataset | # of samples (N) | # of variables (D) | # of clusters (K) | K_0 |
|---------|------------------|--------------------|-------------------|-------|
| Shuttle | 43500 | 9 | 7 | 12 |
| EMG | 59130 | 8 | 6 | 10 |
| MAGIC | 19020 | 10 | 2 | 6 |
| Sloan | 10000 | 16 | 3 | 6 |
| Pulsar | 9273 | 8 | 2 | 6 |
| USPS | 7291 | 3 | 10 | 13 |

privacy or not. For example, following the derivation of the proof of the generalization error bound in [45] and applying the approximating result in [46], we can upper-bound the first term with

$$\frac{2}{N} \left[\frac{c_1 \log_2 (c_2 \hat{\gamma}^2 N)}{\hat{\gamma}^2} + \frac{c_3}{\hat{\gamma}} \log_2 \left(e \left(\frac{(2N-1)\hat{\gamma}}{c_3} + 1 \right) \right) \right] + \frac{2}{N} \left[\log_2 \left(\frac{N^2}{2\delta} \right) + 2 \right]$$

where c_1, c_2, c_3 are constants given as in [45] not relevant to the parameter sets of the MoG and $\hat{\gamma} = \gamma / \|\mathbf{p}\|_W$. Here $\mathbf{p} = [p(\mathbf{x}_1), \dots, p(\mathbf{x}_N)]$ is the N -vector depending on the parameter sets $\{\pi_k, \boldsymbol{\mu}_k, \boldsymbol{\Sigma}_k\}_{k=1, \dots, K}$. Of course, any tighter upper bound of the (differentially private) MoG algorithms can be used to minimize the generalization error bound of the first term, but the second term still needs to be minimized, so we can benefit from using the Morse theory. The results are consistent with the direction of our study to improve the utility while maintaining the privacy of the base methods.

APPENDIX H DETAILS ON THE EXPERIMENTS

We used six datasets: **Shuttle** dataset, EMG physical action (**EMG**) dataset, MAGIC gamma telescope (**MAGIC**) dataset from UCI machine learning repository [47], Sloan digital sky survey (**Sloan**) dataset and Predicting pulsar star (**Pulsar**) dataset from Kaggle competition, and **USPS** [48] dataset. For all datasets, we rescaled each variable in $[-1, 1]$ to ensure DP. **EMG** dataset originally consists of 10 classes, but for convenience, similar actions were removed. For **USPS** dataset, we reduced the dimension from 16×16 to 3 with t-SNE, because the utility of base methods decreases as the dimension increases. More details on the datasets are in Appendix.

Table 2 contains a detailed description of the datasets used for the experiments. The last column in the table, K_0 , denotes the number of sub-clusters generated in the first step of the proposed method.

In addition to the privacy budget ϵ , there are several parameters to be determined. The number of iterations τ_1 and τ_2 were set 10 and 5, respectively, for all experiments. For Algorithm 2, we set the line search parameter $m = 20$, and the small perturbation for finding TEVs ϵ were set to 0.05.

TABLE 3
ARI scores with different numbers of initial sub-clusters for **Magic** dataset.

| $\epsilon \backslash K_0$ | 6 | 10 | 15 | 20 |
|---------------------------|----------|----------|----------|----------|
| 10 | 0.259386 | 0.250220 | 0.248503 | 0.251199 |
| 5 | 0.217444 | 0.215024 | 0.209862 | 0.216947 |
| 2 | 0.083149 | 0.092159 | 0.087595 | 0.096408 |
| 1 | 0.040309 | 0.047554 | 0.040972 | 0.038205 |

APPENDIX I MORE EXPERIMENTAL RESULTS

I.1 Results on k-means clustering

Figure 5 demonstrates the k-means clustering results for six same datasets. The ARI score of **DPLloyd-Morse** is higher than **DPLloyd** in almost all cases. In particular, the ARI score of **DPLloyd-Morse** is more than 0.2 higher than that of **DPLloyd**, which means a substantial improvement. As shown in the figure, non-private **DPLloyd-Morse** performs significantly better than **DPLloyd** in the **Magic** dataset which performs poorly in the k-means algorithm. This shows that Morse theory can improve the utility of k-means algorithm. The difference between ARI scores tends to decrease as epsilon gets smaller, similar to the results for **DPMoG-hard**.

We additionally evaluated the proposed method on a differentially private k-means clustering method in [34], which is a relatively recent study. We denote their method **DPCube** because their method iteratively generates small cubes. Figure 6 demonstrates the results on **DPCube** and **DPCube-Morse**. It is shown that **DPCube-Morse** always shows higher clustering performance than **DPCube** in low-privacy regions. For **EMG**, **DPCube** was better when $\epsilon \leq 2$. However, the difference is not significant because in the case of **EMG**, the scale of the y-axis is very small.

I.2 Effect of increasing sub-clusters

Table 3 shows the clustering results with different numbers of initial sub-clusters for **Magic** dataset with **DPMoG-hard-Morse**. The results show that for **Magic** the clustering performance does not depend on K_0 .

ACKNOWLEDGMENTS

REFERENCES

- [1] G. Kellaris, S. Papadopoulos, and D. Papadias, "Engineering methods for differentially private histograms: Efficiency beyond utility," *IEEE Transactions on Knowledge and Data Engineering*, vol. 31, no. 2, pp. 315–328, 2018.
- [2] G. Acs, L. Melis, C. Castelluccia, and E. De Cristofaro, "Differentially private mixture of generative neural networks," *IEEE Transactions on Knowledge and Data Engineering*, vol. 31, no. 6, pp. 1109–1121, 2018.
- [3] T. Zhu, G. Li, W. Zhou, and S. Y. Philip, "Differentially private data publishing and analysis: A survey," *IEEE Transactions on Knowledge and Data Engineering*, vol. 29, no. 8, pp. 1619–1638, 2017.
- [4] A. Shepitsen, J. Gemmel, B. Mobasher, and R. Burke, "Personalized recommendation in social tagging systems using hierarchical clustering," in *Proceedings of the 2008 ACM conference on Recommender systems*, 2008, pp. 259–266.
- [5] J.-J. Huang, G.-H. Tzeng, and C.-S. Ong, "Marketing segmentation using support vector clustering," *Expert systems with applications*, vol. 32, no. 2, pp. 313–317, 2007.

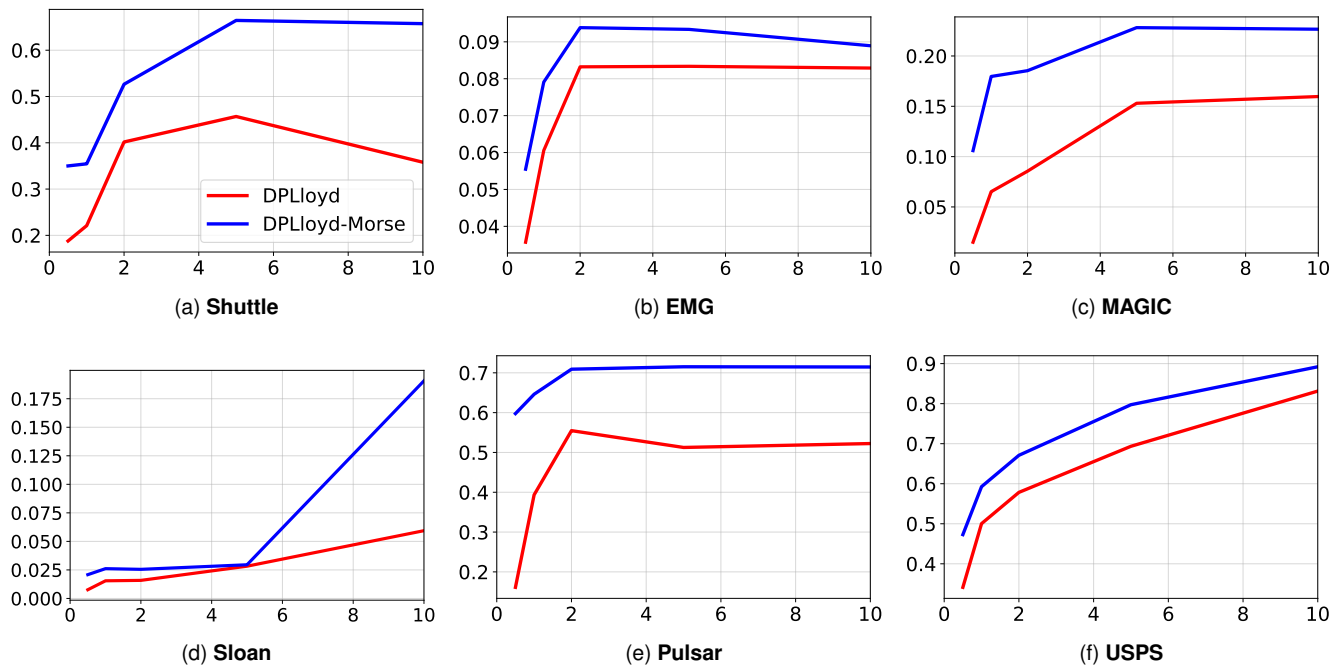


Fig. 5. Clustering results for real-world datasets. The x-axis indicates the noise budget ϵ , and the y-axis indicates the ARI score. The red line shows the performance of **DPLloyd**, and the blue line shows the performance of **DPLloyd-Morse**.

[6] A. S. Sabau, "Survey of clustering based financial fraud detection research," *Informatica Economica*, vol. 16, no. 1, p. 110, 2012.

[7] K.-S. Chuang, H.-L. Tzeng, S. Chen, J. Wu, and T.-J. Chen, "Fuzzy c-means clustering with spatial information for image segmentation," *computerized medical imaging and graphics*, vol. 30, no. 1, pp. 9–15, 2006.

[8] D. Su, J. Cao, N. Li, E. Bertino, and H. Jin, "Differentially private k-means clustering," in *Proceedings of the sixth ACM conference on data and application security and privacy*, 2016, pp. 26–37.

[9] Q. Yu, Y. Luo, C. Chen, and X. Ding, "Outlier-eliminated k-means clustering algorithm based on differential privacy preservation," *Applied Intelligence*, vol. 45, no. 4, pp. 1179–1191, 2016.

[10] C. Xia, J. Hua, W. Tong, and S. Zhong, "Distributed k-means clustering guaranteeing local differential privacy," *Computers & Security*, vol. 90, p. 101699, 2020.

[11] M. Park, J. Foulds, K. Choudhary, and M. Welling, "Dp-em: Differentially private expectation maximization," in *Artificial Intelligence and Statistics*. PMLR, 2017, pp. 896–904.

[12] G. Kamath, O. Sheffet, V. Singhal, and J. Ullman, "Differentially private algorithms for learning mixtures of separated gaussians," *Advances in Neural Information Processing Systems*, vol. 32, pp. 168–180, 2019.

[13] M. A. Pathak and B. Raj, "Large margin gaussian mixture models with differential privacy," *IEEE Transactions on dependable and secure computing*, vol. 9, no. 4, pp. 463–469, 2012.

[14] D. Lee and J. Lee, "Dynamic dissimilarity measure for support-based clustering," *IEEE Transactions on Knowledge and Data Engineering*, vol. 22, no. 6, pp. 900–905, 2009.

[15] C. Dwork, F. McSherry, K. Nissim, and A. Smith, "Calibrating noise to sensitivity in private data analysis," in *Theory of cryptography conference*. Springer, 2006, pp. 265–284.

[16] C. Dwork, A. Roth et al., "The algorithmic foundations of differential privacy," *Found. Trends Theor. Comput. Sci.*, vol. 9, no. 3-4, pp. 211–407, 2014.

[17] M. W. Hirsch, *Differential topology*. Springer Science & Business Media, 2012, vol. 33.

[18] R. Palais and S. Smale, "A generalized morse theory," in *The Collected Papers of Stephen Smale: Volume 2*, 2000, pp. 503–510.

[19] H. T. Jongen, P. Jonker, and F. Twilt, *Nonlinear optimization in IRN*. P. Lang Publishing Co., 1987.

[20] S. Smale, "On gradient dynamical systems," *Annals of Mathematics*, pp. 199–206, 1961.

[21] J. Guckenheimer and P. Holmes, *Nonlinear oscillations, dynamical systems, and bifurcations of vector fields*. Springer Science & Business Media, 2013, vol. 42.

[22] H. K. Khalil, "Nonlinear systems third edition," *Patience Hall*, vol. 115, 2002.

[23] H.-D. Chiang and L. Fekih-Ahmed, "Quasi-stability regions of nonlinear dynamical systems: Theory," *IEEE Transactions on Circuits and Systems I: Fundamental Theory and Applications*, vol. 43, no. 8, pp. 627–635, 1996.

[24] J. Lee and H.-D. Chiang, "A dynamical trajectory-based methodology for systematically computing multiple optimal solutions of general nonlinear programming problems," *IEEE Transactions on Automatic Control*, vol. 49, no. 6, pp. 888–899, 2004.

[25] A. Blum, C. Dwork, F. McSherry, and K. Nissim, "Practical privacy: the sulq framework," in *Proceedings of the twenty-fourth ACM SIGMOD-SIGACT-SIGART symposium on Principles of database systems*, 2005, pp. 128–138.

[26] K. Nissim, S. Raskhodnikova, and A. Smith, "Smooth sensitivity and sampling in private data analysis," in *Proceedings of the thirtieth annual ACM symposium on Theory of computing*, 2007, pp. 75–84.

[27] D. Feldman, A. Fiat, H. Kaplan, and K. Nissim, "Private coresets," in *Proceedings of the forty-first annual ACM symposium on Theory of computing*, 2009, pp. 361–370.

[28] E. Cohen, H. Kaplan, Y. Mansour, U. Stemmer, and E. Tsfadia, "Differentially-private clustering of easy instances," in *International Conference on Machine Learning*. PMLR, 2021, pp. 2049–2059.

[29] M. Shechner, O. Sheffet, and U. Stemmer, "Private k-means clustering with stability assumptions," in *International Conference on Artificial Intelligence and Statistics*. PMLR, 2020, pp. 2518–2528.

[30] M. Kearns, Y. Mansour, and A. Y. Ng, "An information-theoretic analysis of hard and soft assignment methods for clustering," in *Learning in graphical models*. Springer, 1998, pp. 495–520.

[31] G. Celeux and G. Govaert, "A classification em algorithm for clustering and two stochastic versions," *Computational statistics & Data analysis*, vol. 14, no. 3, pp. 315–332, 1992.

[32] A. Samé, C. Ambroise, and G. Govaert, "An online classification em algorithm based on the mixture model," *Statistics and Computing*, vol. 17, no. 3, pp. 209–218, 2007.

[33] D. Lee, J. Lee, and Y.-G. Yoon, "A quadratic string adapted barrier exploring method for locating transition states," *Computer physics communications*, vol. 177, no. 1-2, pp. 218–218, 2007.

[34] M.-F. Balcan, T. Dick, Y. Liang, W. Mou, and H. Zhang, "Differentially private clustering in high-dimensional euclidean spaces,"

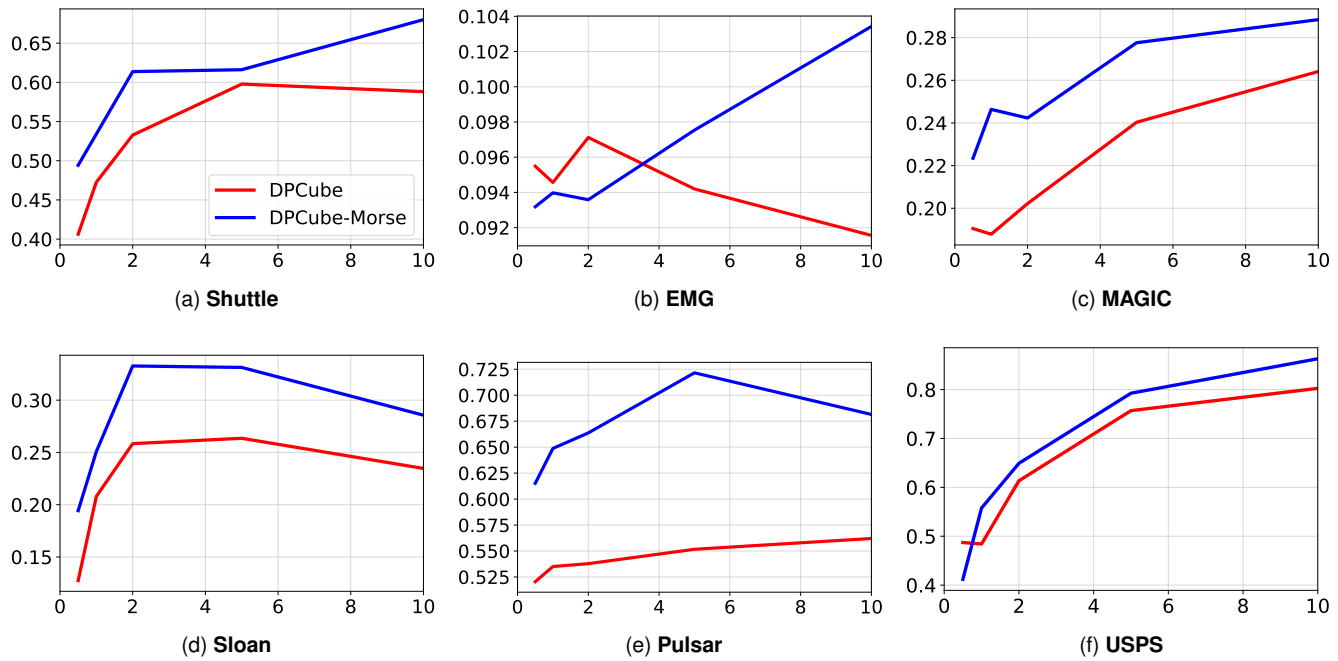


Fig. 6. Clustering results for real-world datasets. The x-axis indicates the noise budget ϵ , and the y-axis indicates the ARI score. The red line shows the performance of **DPCube**, and the blue line shows the performance of **DPCube-Morse**.

in *International Conference on Machine Learning*. PMLR, 2017, pp. 322–331.

[35] Z. Huang and J. Liu, “Optimal differentially private algorithms for k-means clustering,” in *Proceedings of the 37th ACM SIGMOD-SIGACT-SIGAI Symposium on Principles of Database Systems*, 2018, pp. 395–408.

[36] L. Ni, C. Li, X. Wang, H. Jiang, and J. Yu, “Dp-mcdbcscan: Differential privacy preserving multi-core dbscan clustering for network user data,” *IEEE Access*, vol. 6, pp. 21 053–21 063, 2018.

[37] W.-m. Wu and H.-k. Huang, “A dp-dbscan clustering algorithm based on differential privacy preserving,” *Computer Engineering and Science*, vol. 37, no. 4, pp. 830–834, 2015.

[38] Y. Zhang and J. Han, “Differential privacy fuzzy c-means clustering algorithm based on gaussian kernel function,” *Plos one*, vol. 16, no. 3, p. e0248737, 2021.

[39] M. Bun and T. Steinke, “Concentrated differential privacy: Simplifications, extensions, and lower bounds,” in *Theory of Cryptography Conference*. Springer, 2016, pp. 635–658.

[40] J. Lee and D. Lee, “Dynamic characterization of cluster structures for robust and inductive support vector clustering,” *IEEE Transactions on Pattern Analysis and Machine Intelligence*, vol. 28, no. 11, pp. 1869–1874, 2006.

[41] H. K. Khalil, “1992, nonlinear systems, macmillan, new york.”

[42] E. Suhubi, “Nonlinear oscillations, dynamical systems, and bifurcations of vector fields: Applied mathematical science, vol. 42, j. guckenheimer and p. holmes, springer-verlag, new york, berlin, heidelberg, tokyo (1983). xvi+ 453 pp., 206 figs, dm 104,” 1988.

[43] J. A. Hartigan, *Clustering algorithms*. John Wiley & Sons, Inc., 1975.

[44] M. Seeger, “Learning with labeled and unlabeled data,” Tech. Rep., 2000.

[45] B. Schölkopf, J. C. Platt, J. Shawe-Taylor, A. J. Smola, and R. C. Williamson, “Estimating the support of a high-dimensional distribution,” *Neural computation*, vol. 13, no. 7, pp. 1443–1471, 2001.

[46] D. Lee, K.-H. Jung, and J. Lee, “Constructing sparse kernel machines using attractors,” *IEEE transactions on neural networks*, vol. 20, no. 4, pp. 721–729, 2009.

[47] D. Dua and C. Graff, “UCI machine learning repository,” 2017. [Online]. Available: <http://archive.ics.uci.edu/ml>

[48] J. J. Hull, “A database for handwritten text recognition research,” *IEEE Transactions on pattern analysis and machine intelligence*, vol. 16, no. 5, pp. 550–554, 1994.